

Supplementary Information for

TiS₃ Sheet Based Van der Waals Heterostructures with Tunable Schottky Barrier

Jie Liu ^{1,2,3}, Yaguang Guo^{1,2,3}, Fancy Qian Wang^{1,2,3}, and Qian Wang^{1,2,3}

¹Center for Applied Physics and Technology, Peking University, Beijing 100871, China

²Department of Materials Science and Engineering, College of Engineering, Peking University, Beijing 100871, China

³Collaborative Innovation Center of IFSA (CICIFSA), Shanghai JiaoTong University, Shanghai 200240, China

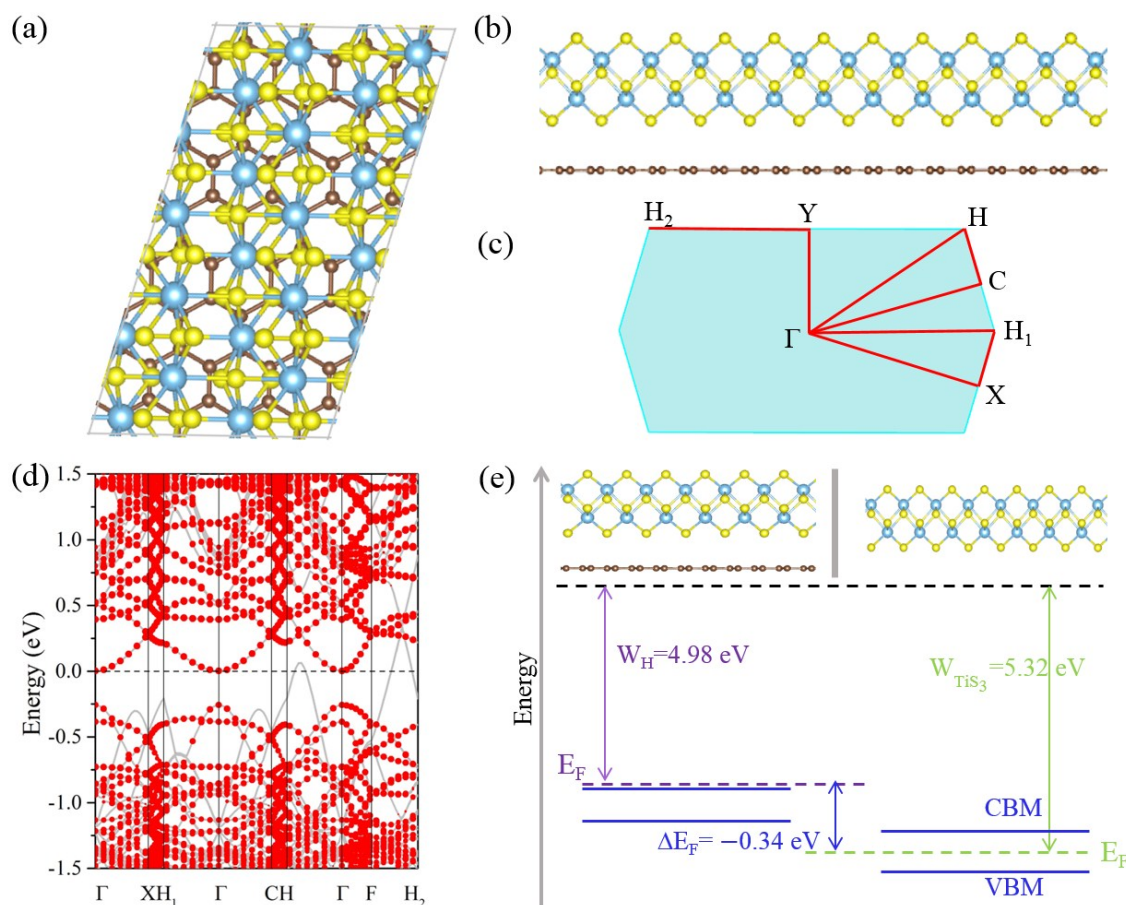


Fig. S1 (a) Top and (b) side views of the TiS₃/G heterostructure of Case 2. (c) The First Brillouin zone and high-symmetry q-point paths: Γ (0.0, 0.0, 0.0) → X(0.5, 0.0, 0.0), H(0.5, 0.5, 0.0), H₁(0.5, 0.0, 0.0), C(0.0, 0.5, 0.0), Y(0.0, 0.0, 0.5), and H₂(0.0, 0.0, 0.0). (d) Energy band structure plot showing Energy (eV) versus path from Γ to H₂. (e) Energy band diagram showing the band gap $W_H = 4.98$ eV for the top layer and $W_{TiS_3} = 5.32$ eV for the bottom layer, with Fermi levels E_F and VBM/CBM levels.

$0.0) \rightarrow H_1(0.543, 0.272, 0.0) \rightarrow \Gamma(0.0, 0.0, 0.0) \rightarrow C(0.5, 0.5, 0.0) \rightarrow H(0.457, 0.728, 0.0) \rightarrow \Gamma(0.0, 0.0, 0.0) \rightarrow Y(0.0, 0.5, 0.0) \rightarrow H_2(-0.457, 0.272, 0.0)$. (d) Electronic band structure projected on the TiS_3 layer. (e) Schematic depictions of the band alignment. These results are all calculated at the GGA-PBE level.

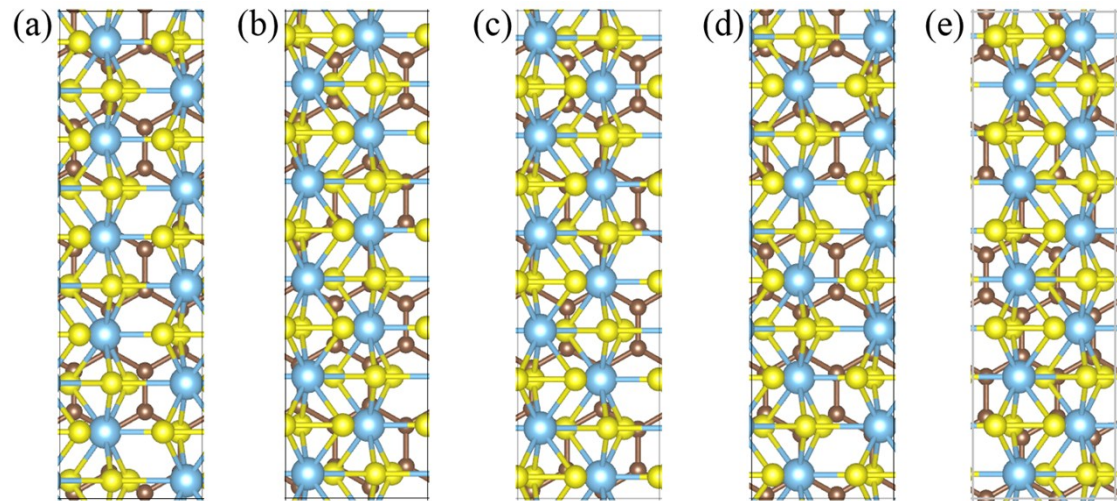


Fig. S2 Top views of the TiS_3 /G heterostructure in five different stacking patterns (S1–S5). The titanium, sulfur, and carbon atoms are represented by the cyan, yellow and dark red spheres, respectively.

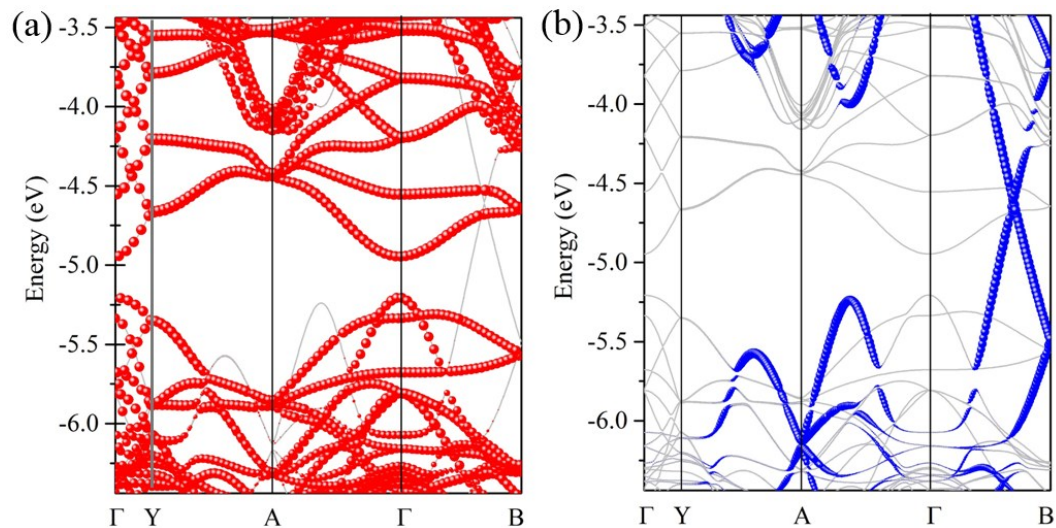


Fig. S3 Electronic band structure of the TiS_3 /graphene heterostructure aligned with respect to the vacuum level projected on (a) the TiS_3 layer, and (b) the graphene sheet calculated by using the GGA–PBE functional.

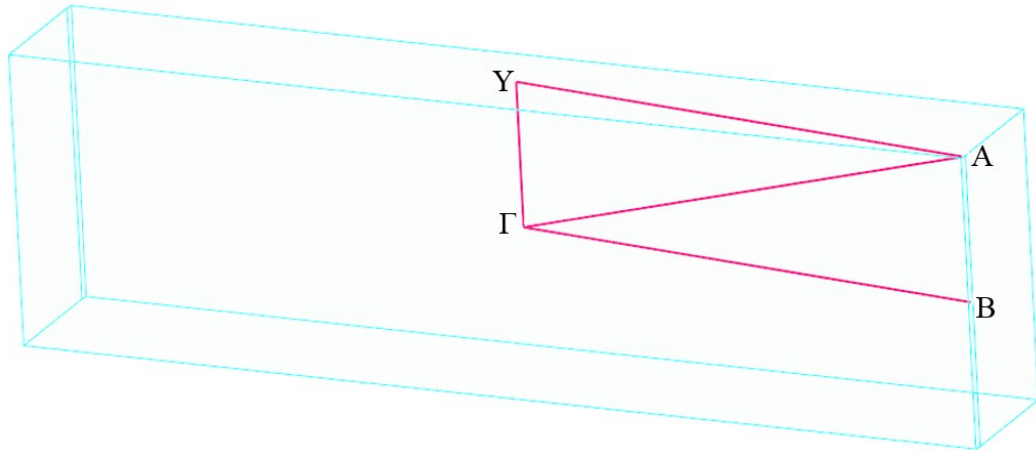


Fig. S4 The first Brillouin zone and high-symmetry q -point paths: $\Gamma(0.0, 0.0, 0.0) \rightarrow Y(0.0, 0.5, 0.0) \rightarrow A(0.5, 0.5, 0.0) \rightarrow \Gamma(0.0, 0.0, 0.0) \rightarrow B(0.5, 0.5, 0.0)$ for the TiS_3/G heterostructure.

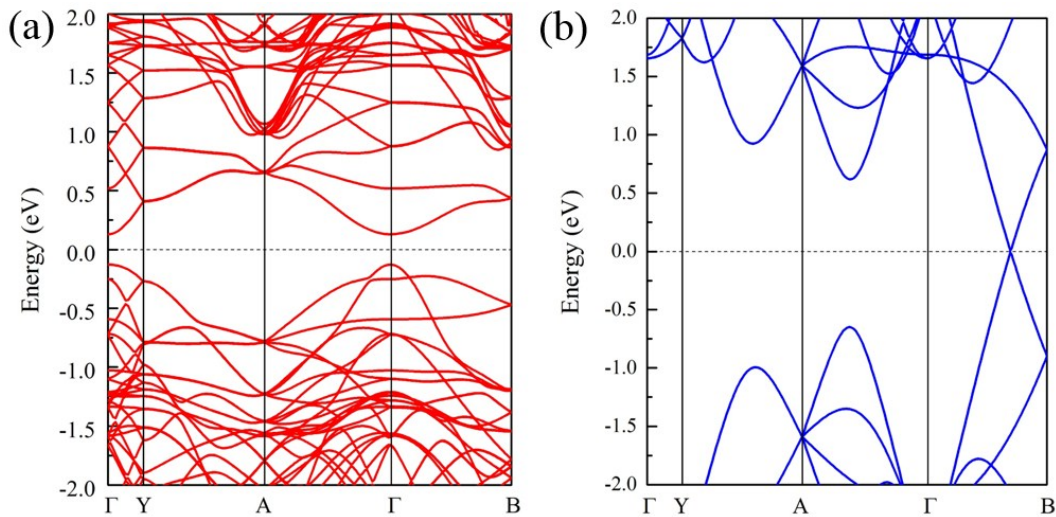


Fig. S5 Band structures of the isolated (c) TiS_3 monolayer and (d) graphene monolayer calculated by the GGA–PBE functional using the undistorted supercell of the two 2D materials.

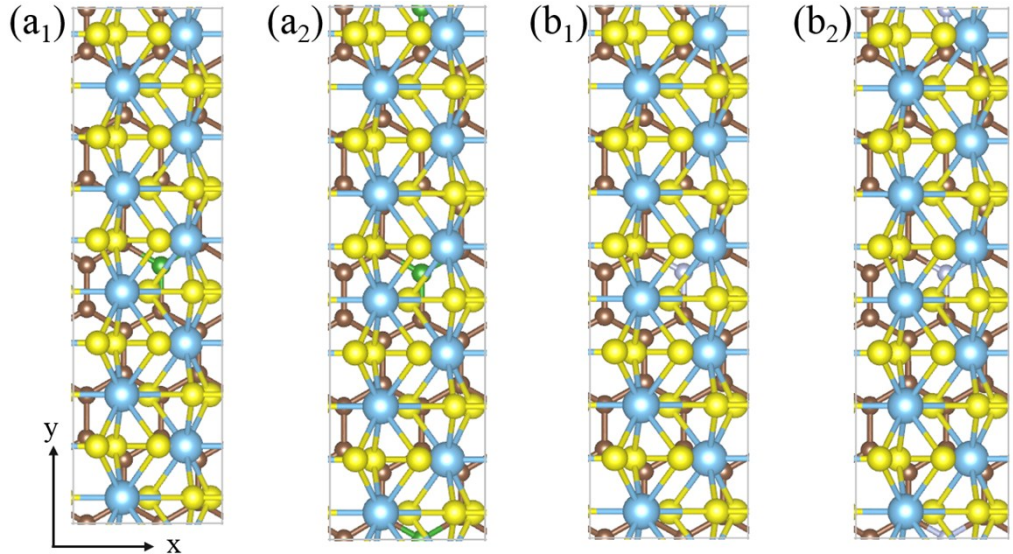


Fig. S6 Top views of the heterostructures formed by (a₁)–(a₂) TiS₃ and B-doped graphene and (b₁)-(b₂) TiS₃ and N-doped graphene with the concentrations of (a₁)-(b₁) 1/32 and (a₂)-(b₂) 1/16. For a clear view, green and gray spheres denote the boron and nitrogen atoms, respectively.

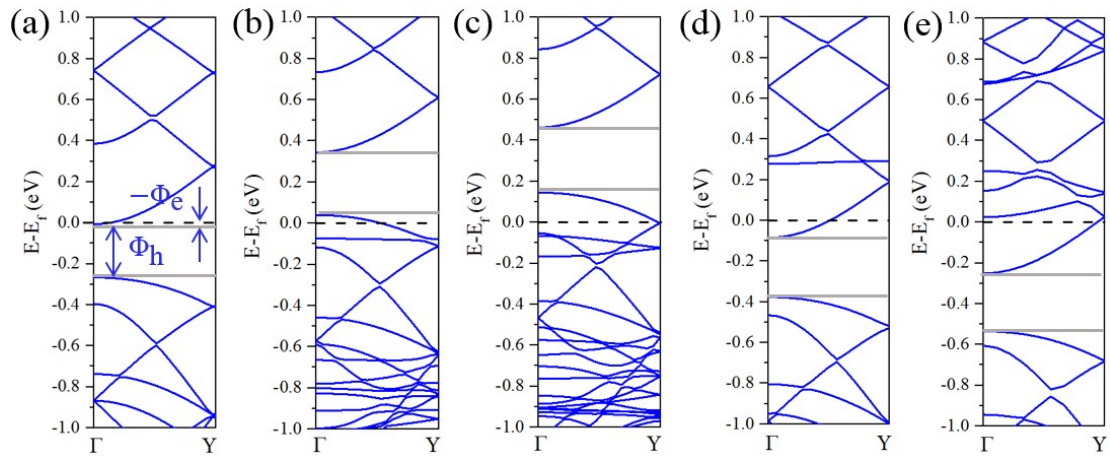


Fig. S7 Schematic depictions of the SBHs calculated by using the PBE-GGA functional for the Van der Waals heterostructure constructed by TiS₃ layer contacted with (a) pristine graphene, (b) 1/32 B-doped, (c) 1/16 B-doped, (d) 1/32 N-doped, and (e) 1/16 N-doped graphene.

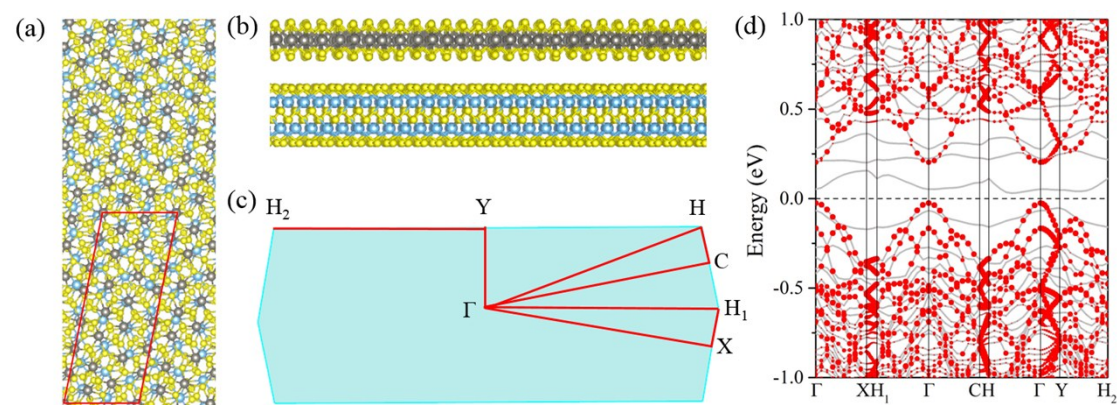
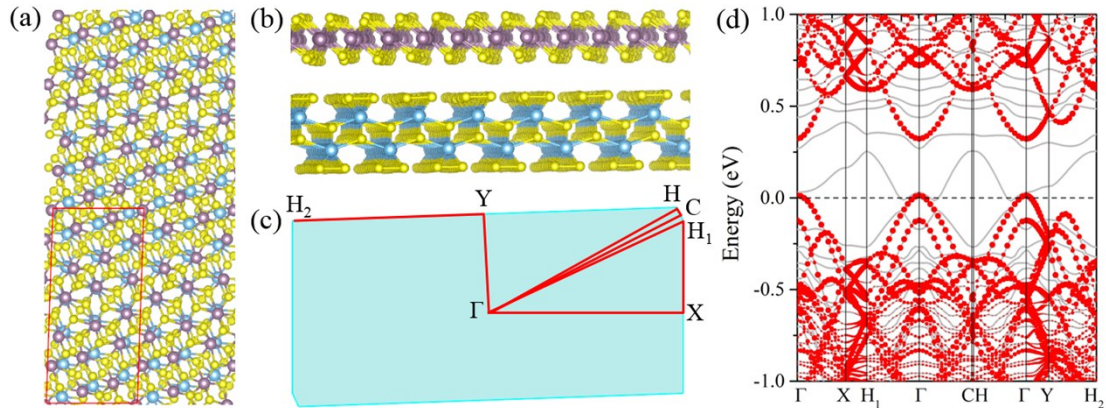


Fig. S9 (a) Top and (b) side views of the $\text{TiS}_3/\text{T}-\text{WS}_2$ heterostructure. (c) The first Brillouin zone and the high-symmetry q -point paths: $\Gamma(0.0, 0.0, 0.0) \rightarrow X(0.5, 0.0, 0.0) \rightarrow H_1(0.518, 0.276, 0.0) \rightarrow \Gamma(0.0, 0.0, 0.0) \rightarrow C(0.5, 0.5, 0.0) \rightarrow H(0.482, 0.724, 0.0) \rightarrow \Gamma(0.0, 0.0, 0.0) \rightarrow Y(0.0, 0.5, 0.0) \rightarrow H_2(-0.482, 0.276, 0.0)$. (d) Electronic band structure projected on the TiS_3 layer calculated at the GGA-PBE level.

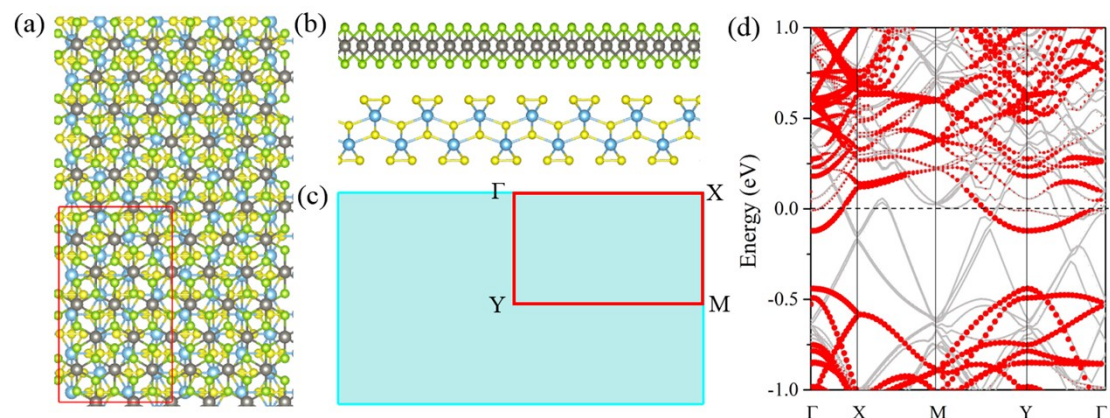
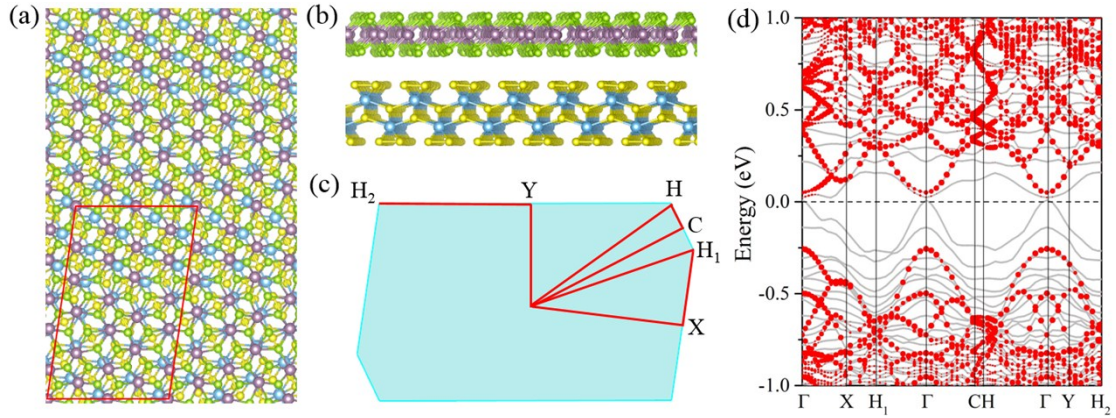


Fig. S11 (a) Top and (b) side views of the $\text{TiS}_3/\text{T}-\text{WSe}_2$ heterostructure. (c) The first Brillouin zone and the high-symmetry q -point paths: $\Gamma(0.0, 0.0, 0.0) \rightarrow X(0.5, 0.0, 0.0) \rightarrow M(0.5, 0.5, 0.0) \rightarrow Y(0.0, 0.5, 0.0) \rightarrow \Gamma(0.0, 0.0, 0.0)$. (d) Electronic band structure projected on the TiS_3 layer calculated at the GGA-PBE level.

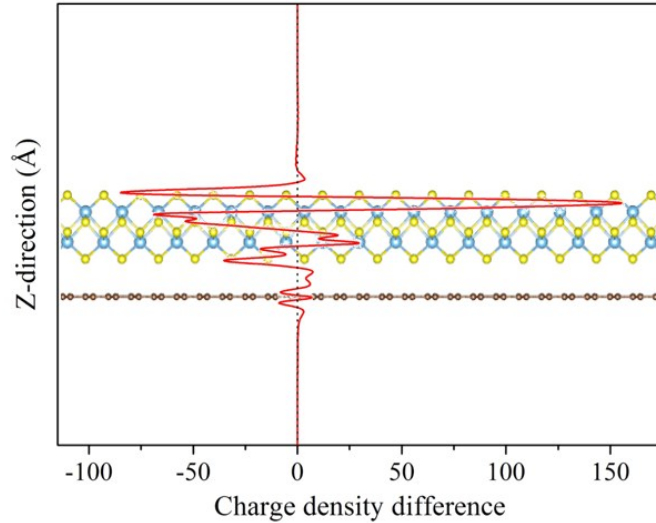


Fig. S12 Charge density difference (averaged in the plane parallel to the interface) of the TiS_3/G heterostructure.

Table S1 Comparison of the binding energy (E_b), band bending (ΔE_F), and Schottky barrier height (Φ_e for electron and Φ_h for hole) between case 1 and case2.

	E_b	ΔE_F	Φ_e	Φ_h
Case 1	65 meV	-0.38	-0.01	0.23
Case 2	66 meV	-0.34	-0.01	0.22

Table S2 The relative energies (ΔE in meV/supercell) of the five configurations (S1–S5) of the TiS_3/G heterostructure in different stacking patterns.

	S1	S2	S3	S4	S5
ΔE	1.9	0.5	10.9	0.1	0

Table S3 Comparison of the Schottky barrier heights calculated by using the HSE06 and GGA-PBE functionals of the Van der Waals heterostructures constructed by TiS₃ layer contact with 1/16 B-doped, 1/32 B-doped, pristine, 1/32 N-doped, 1/16 N-doped graphene.

		B (1/16)	B (1/32)	pristine	N (1/32)	N (1/16)
GGA-PBE	Φ_e	0.45	0.34	-0.01	-0.09	-0.26
	Φ_h	-0.14	-0.04	0.24	0.38	0.53
HSE06	Φ_e	0.85	0.46	0.25	-0.09	-0.14
	Φ_h	0.23	0.58	0.76	1.09	1.14

Table S4 Lattice parameters of the TiS₃ and the T-MX₂ (M=Mo or W, X= S or Se) supercells. u_i , v_i , and γ_i , represent the lattice constants (in Å) and the angle between the vectors (in degree), respectively. u_{I_2} (v_{I_2} or γ_{I_2}) and N represent the lattice

	TiS ₃ a=4.99 Å, b=3.39 Å, $\alpha=90^\circ$			MX ₂			Mismatch (%)			N
	u_I	v_I	γ_I	u_2	v_2	γ_2	u_{I_2}	v_{I_2}	γ_{I_2}	
T-MoS ₂ a=3.19 Å, b=3.19 Å, $\alpha=120^\circ$	8.44	17.75	88.05	8.41	18.08	87.82	0.30	1.86	0.26	123
T-WS ₂ a=3.17 Å, b=3.17 Å, $\alpha=120^\circ$	8.41	22.38	80.63	8.39	22.19	79.11	0.30	0.90	1.93	151
T-MoSe ₂ a=3.33 Å, b=3.33 Å, $\alpha=120^\circ$	11.32	18.08	81.96	11.25	18.08	81.05	0.62	0.02	1.12	162
T-WSe ₂ a=3.26 Å, b=3.26 Å, $\alpha=120^\circ$	9.97	16.93	90.00	9.78	16.95	90.00	1.93	0.08	0.00	134

mismatch and the total number of atoms of the heterostructure.